Polymer Chemistry

RSC Publishing

PAPER

View Article Online
View Journal | View Issue

# Visualization of the crucial step in SET-LRP

Cite this: *Polym. Chem.*, 2013, **4**, 1635

Martin E. Levere, Nga H. Nguyen, Xuefei Leng and Virgil Percec*

The crucial step in SET-LRP is the disproportionation of the CuX generated by activation with Cu(0) wire or powder, into *nascent*, extremely reactive Cu(0) nanoparticles, and $CuX_2$. *Nascent* Cu(0) activates the initiator and dormant chains *via* a heterogeneous single-electron transfer (SET) mechanism. Here we report model reactions visualizing the disproportionation of CuBr and activation by *nascent* Cu(0) in protic, dipolar aprotic, and nonpolar solvents, and in protic, polar and nonpolar monomers. The *nascent* Cu(0) nanoparticles and the green/blue color of the solution of $CuBr_2$/N-ligand were visible, demonstrating that disproportionation occurs under all SET-LRP and many ATRP conditions. Unexpectedly, *nascent* Cu(0) nanoparticles and insoluble $CuBr_2$ were also formed *via* a *surface disproportionation* of CuBr/$Me_6$-TREN in a range of nonpolar solvents and monomers. The effect of solvent polarity on the rate of SET activation was visualized by adding methyl 2-bromopropionate (MBP) initiator to the disproportionation mixture and monitoring the disappearance of the *nascent* Cu(0) nanoparticles. The consumption of *nascent* Cu(0) was extremely rapid in DMSO, fast in MeCN, and slower in toluene. This trend confirms the expected dependence of SET activation on solvent polarity. The enhanced stabilization of Cu(0) nanoparticles in DMSO compared to MeOH was visualized, and used to explain the synergistic solvent effect in DMSO–MeOH and other solvent–monomer mixtures. Visualization of the disproportionation and activation also explains the rate acceleration in *CuX-catalyzed ATRP in polar media* in which the active catalyst is most likely the extremely reactive *nascent* Cu(0) generated by disproportionation, and therefore, rapidly discriminates between SET-LRP and ATRP.

Received 10th December 2012
Accepted 16th December 2012

DOI: 10.1039/c2py21084c

**www.rsc.org/polymers**



## Introduction

Single-electron transfer living radical polymerization (SET-LRP) has its roots in earlier efforts to develop a metal-catalyzed living radical polymerization (LRP) of vinyl chloride (VC).[1] At that time, it was reported that even the most active CuX complexes failed to polymerize VC under atom transfer radical polymerization (ATRP) because of the inert –CHClX end group of poly(vinyl chloride) (PVC) that cannot be reactivated.[2] In addition, in free radical polymerization of VC, chain transfer to polymer is a more dominant process than bimolecular termination. This prevents the establishment of the persistent radical effect (PRE)[3] in which a small extent of radical dimerization accumulates $CuX_2$ deactivator and shifts the equilibrium between the active and dormant species toward the dormant species. However, it was discovered that Cu(0)–2,2′-bipyridine (bpy) showed remarkable activity for reinitiation of –CHClX chain-ends of PVC compared to CuX species.[1] By exploiting the disproportionation of CuX into Cu(0) and $CuX_2$ in polar media these studies further evolved into single-electron transfer degenerative transfer living radical polymerization (SET-DTLRP).[4] In SET-DTLRP, both activation and deactivation are provided by a competition between the SET from Cu(0) and degenerative chain transfer mechanisms, and by $CuX_2$/L generated by the disproportionation of CuX without the need for PRE.[4] Under suitable conditions such as the use of a polar solvent, DMSO, when activation and deactivation are faster than the degenerative chain-transfer, the DT part of SET-DTLRP is eliminated, and the newly elaborated LRP becomes SET-LRP.[5] Since its discovery, SET-LRP has proven to be a robust and versatile method for the ultrafast synthesis of vinyl polymers using incredibly low catalyst loadings under mild reaction conditions.[5] SET-LRP exhibits quantitative initiator efficiency, and as such facilitates the synthesis of ultrahigh molecular weight poly(acrylates) in less than 12 h at room temperature.[5] Subsequent reports have expanded this method for the synthesis of well-defined polymers from a large diversity of monomers including acrylates,[5,6] acrylamides[7,8] and methacrylates[5,9] with different polarity profiles, and of perfectly functional homopolymers, block copolymers and high-order multiblock copolymers even at complete monomer conversion.[10]

Scheme 1 shows the proposed mechanism of SET-LRP.[4,5] SET-LRP proceeds by a heterogeneous single-electron transfer (SET) mechanism in which the electron-donor Cu(0) activates the electro-acceptor alkyl halide initiator and dormant propagating species to generate CuX and the propagating radical.[4,5] Depending on the substrate and the nature of the leaving group,

*Roy & Diana Vagelos Laboratories, Department of Chemistry, University of Pennsylvania, Philadelphia, Pennsylvania 19104-6323, USA. E-mail: percec@sas.upenn.edu*

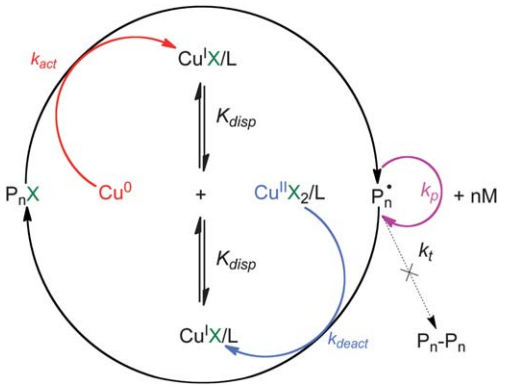


**Scheme 1** Proposed mechanism of SET-LRP.[4,5]

the electron transfer and subsequent fragmentation of the resulting radical-anion can be concerted or stepwise.[4,5] Thus the crucial step in SET-LRP is the self-regulated disproportionation of CuX that generates *in situ* both the extremely reactive *nascent* Cu(0) activator and $CuX_2$/L deactivator required for the reversible termination step.[4,5] This ligand–solvent-mediated disproportionation of CuX eliminates the need for the undesirable bimolecular termination to accumulate the excess of $CuX_2$ deactivator, and therefore, the classic persistent radical effect (PRE)[3] is no longer required.[11]

The mechanism of SET-LRP can be considered a complex system,[12] since it responds to a series of "environmental conditions" that include solvent polarity,[13] nature of ligand and its concentration,[14] the extent of disproportionation by the solvent–ligand combination,[15] its ability to stabilize Cu(0) colloidal particles and self-control the reactivity of *nascent* Cu(0).[5b] In this article, model disproportionation experiments of CuBr were performed in a series of organic solvents and monomers with different polarity profiles and characterized by direct visualization that was complemented by UV-vis spectroscopy. These visual observations will be used to support previous results reported from our and other laboratories, such as the loss of chain-end functionality and limited conversion in Cu(0)-mediated polymerizations in nonpolar solvents, and challenges in polymerizing certain classes of monomers due to the limited solubility of the $CuX_2$ deactivating species. The Cu(0)-mediated activation of an alkyl halide initiator was also visualized to provide further mechanistic insights into the cooperative and synergistic solvent effects and solvent polarity on the activation step of SET-LRP.

## Results and discussion

### Selection of the reaction conditions and methods

The disproportionation of CuBr/N-ligand and activation with the resulting Cu(0) nanoparticles by addition of methyl 2-bromopropionate (MBP) initiator were performed in sealable airtight quartz UV-vis cuvettes with screw cap fitting. To ensure visualization, a higher concentration of CuBr than usually employed in SET-LRP was used (16.5 mM) in 1.8 mL of deoxygenated solvent. Upon addition of the deoxygenated solvent–ligand mixture into the UV-vis cuvettes containing CuBr in an inert atmosphere in the glovebox, the reactions were monitored for a period that was greater than the timescale of the polymerization reaction, and pictures were taken at different times. A [CuBr]/[N-ligand] molar ratio of 1/1 (1 equivalent of $Me_6$-TREN) was chosen for all disproportionation reactions except for those in DMSO, in which a [CuBr]/[N-ligand] molar ratio of 1/0.5 (0.5 equivalent of $Me_6$-TREN) has previously been reported to provide the maximum extent of disproportionation. In all cases, 1 to 2 min vortex mixing was applied immediately after mixing of reagents in the UV-vis cuvette cells. The disproportionation of CuBr/N-ligand was demonstrated by the observation of the insoluble Cu(0) nanoparticles, and by the color change from colorless to green/blue depending on solvent and ligand combination. The disproportionation was also monitored by the UV-vis absorbance corresponding to the *in situ* generated $CuBr_2$/N-ligand complex. Activation of MBP by the *nascent* Cu(0) nanoparticles generated from the disproportionation was visualized by monitoring the disappearance of the *nascent* Cu(0) nanoparticles.

### Disproportionation of CuBr/N-ligands in dipolar aprotic solvents

The disproportionation of CuX in $H_2O$ has been known for over 100 years,[16] to proceed with an equilibrium constant of $0.89 \times 10^6$ to $5.8 \times 10^7$ even in the absence of a ligand that preferentially stabilizes $CuX_2$. In organic solvents, the presence of $CuX_2$-stabilizing N-ligands such as tris[2-(dimethylamino)ethyl]amine ($Me_6$-TREN) or tris(2-aminoethyl)amine (TREN)[14a] enhances the disproportionation of CuX up to four orders of magnitude compared to the results in the absence of a ligand in the same solvent.[15] Fig. 1 shows the disproportionation of CuBr in DMSO at different ligand concentrations: [CuBr]/[$Me_6$-TREN] = 1/0.5 and 1/1. In both cases disproportionation of CuBr/$Me_6$-TREN in DMSO occurred immediately upon mixing. This was indicated by the formation of Cu(0) nanoparticles and a faint green color corresponding to $CuBr_2$/$Me_6$-TREN complex in DMSO. It was observed that DMSO stabilizes colloidal Cu(0) particles, resulting in a red suspension shown in Fig. 1. Comparing Fig. 1a and

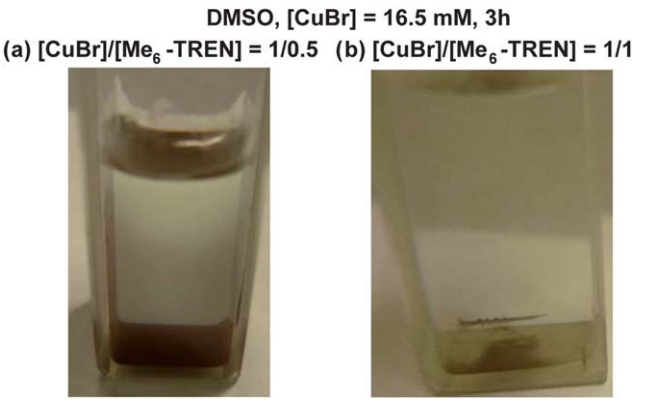


**Fig. 1** Visual observation of the disproportionation of CuBr in DMSO with 0.5 equivalent (a); and 1 equivalent (b) of $Me_6$-TREN after 3 h at 25 °C. Conditions: DMSO = 1.8 mL; (a) [CuBr]/[$Me_6$-TREN] = 1/0.5 and (b) [CuBr]/[$Me_6$-TREN] = 1/1.

b, it can be visually observed that the amount of Cu(0) generated at 0.5 equivalent of $Me_6$-TREN is higher than that obtained at 1 equivalent of $Me_6$-TREN. This can be translated to a higher $K_{dis}$ at 0.5 equivalent of $Me_6$-TREN with respect to CuBr concentration in DMSO. This result is in agreement with a previous UV-vis study that showed that the maximum extent of disproportionation occurred at this CuBr/ligand molar ratio in DMSO.[15]

A survey of different combinations of solvents and ligands showed that other dipolar aprotic solvents such as propylene carbonate, DMF, ionic liquids, and ligands (TREN and $Me_6$-TREN) also promote the disproportionation of CuBr to Cu(0) and $CuBr_2$ (Fig. 2). On the other hand, in a polar solvent such as MeCN, which is a good stabilizing ligand for CuX, disproportionation does not occur under these conditions since no insoluble Cu(0) nanoparticles were observed. This result is in agreement with previous UV-vis studies (Fig. 2).[5,15]

### Disproportionation of CuBr/N-ligands in protic solvents

The disproportionation of CuBr/$Me_6$-TREN was also investigated in a series of protic solvents including fluorinated alcohols at [CuBr]/[$Me_6$-TREN] = 1/1 (Fig. 3). With the exception of hexafluoroisopropanol, $(CF_3)_2CHOH$, disproportionation of CuBr/$Me_6$-TREN can be visually observed in a wide range of commercially available alcohols, indicated by the formation of Cu(0) nanoparticles and a green color corresponding to the solution of $CuBr_2$. In *t*-butanol, $Me_6$-TREN mediates the disproportionation of CuBr. However, the presence of a green precipitate corresponding to $CuBr_2$/$Me_6$-TREN indicates that this complex is not soluble in *t*-butanol.

In all protic solvents such as MeOH, *nascent* Cu(0) formed by disproportionation of CuBr/$Me_6$-TREN agglomerates and precipitates rapidly resulting in a clear solution with sedimentation of Cu(0) nanoparticles at the bottom of the UV-vis cuvette cells (Fig. 4b). This is in contrast to other dipolar aprotic solvents such as DMSO, DMF or ionic liquids which stabilize the formation of the suspension of the Cu(0) colloidal nanoparticles (Fig. 4a). Dynamic Light Scattering (DLS) and Transmission Electron Microscopy (TEM) analyses of the disproportionation mixture in DMSO confirmed the presence of very small Cu(0) nanoparticles (7 nm over a distribution of 1200 particles),[6c,17] while only agglomeration of larger Cu(0) nanoparticles was observed in MeOH.[15]

A combination of protic solvents such as MeOH or binary mixtures of MeOH with $H_2O$ also promotes the disproportionation of CuBr in the presence of other N-ligands such as bpy (Fig. 5). Upon dissolution of CuBr–bpy in MeOH and MeOH + 50% $H_2O$ at 25 °C, insoluble Cu(0) nanoparticles were clearly visible within 10 min (Fig. 5), and therefore visually demonstrated for the first time that of CuBr–bpy complex disproportionates in MeOH and in binary mixtures of MeOH with $H_2O$ at 25 °C. A deep red color was also observed in previous reactions where bpy has been used as a ligand.[18]

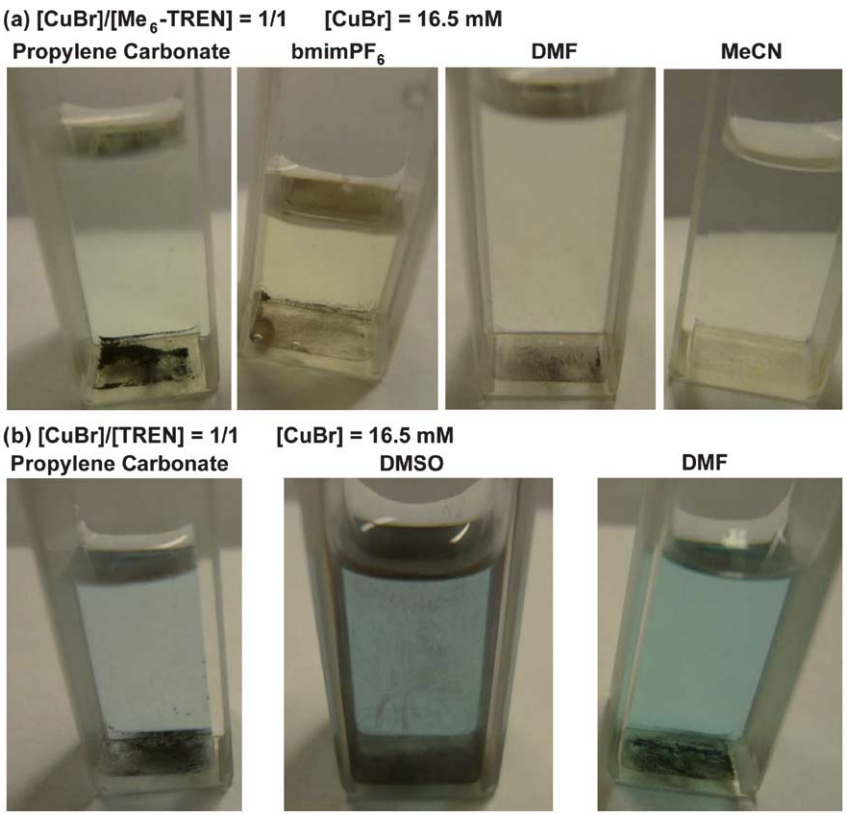


**Fig. 2** Visual observation of Cu(0) nanoparticles and $CuBr_2$ generated from the disproportionation of CuBr in polar aprotic solvents in the presence of $Me_6$-TREN (a); and TREN (b). Conditions: solvent = 1.8 mL; [CuBr]/[N-ligand] = 1/1. Pictures were taken 10 min after mixing the reagents.

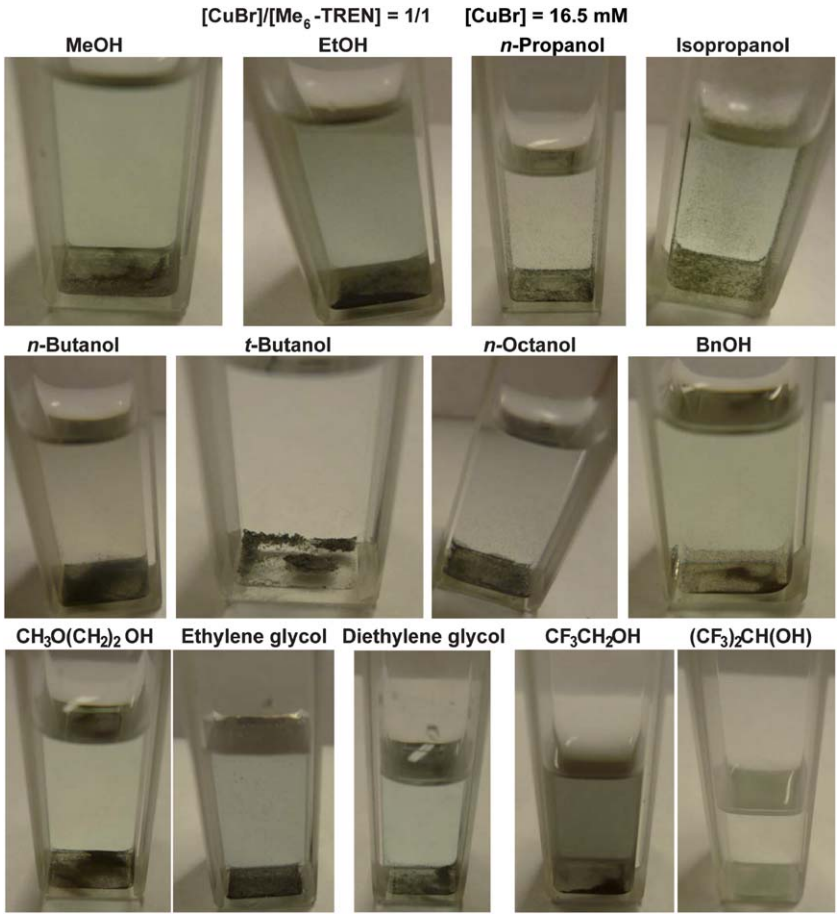


**Fig. 3** Visual observation of Cu(0) nanoparticles and $CuBr_2$ generated from the disproportionation of $CuBr/Me_6$-TREN in a range of alcohols at 25 °C. Conditions: solvent = 1.8 mL, [CuBr] = 16.5 mM, $[CuBr]/[Me_6\text{-TREN}] = 1/1$. Pictures were taken 10 min after mixing the reagents.

### Disproportionation of $CuBr/Me_6$-TREN in nonpolar solvents

The disproportionation of $CuX–Me_6$-TREN in polar solvents has been extensively investigated using different techniques.[5,15] However, the use of nonpolar solvents to mediate the disproportionation process has not been explored. It was suggested from the kinetic and simulation experiments that the amount of $H_2O$ available in commercial solvents is sufficient to induce the disproportionation of CuX to Cu(0) and $CuX_2$.[19] To test this hypothesis, the disproportionation of CuBr was performed in a range of nonpolar solvents in the presence of $Me_6$-TREN (Fig. 6). Unexpectedly, all nonpolar solvents investigated disproportionate CuBr, as shown by the formation of Cu(0) nanoparticles on the surface of CuBr. This discovery has extremely important implications for the design and elaboration of conditions required for the effective SET-LRP of nonpolar monomers.

Interestingly, disproportionation was even observed in hydrocarbon solvents such as hexane, toluene (Fig. 6) and, as shown later, in styrene (Fig. 7b). However, unlike the disproportionation in polar solvents, the formation of Cu(0) nanoparticles was accompanied with a colorless reaction mixture which suggests the absence of soluble $CuBr_2/Me_6$-TREN complex in these solvents even after vortex mixing. This is supported by UV-vis spectroscopy experiments before and after vortex mixing, as shown later in Fig. 9b, which showed the absence of the absorbance of $CuBr_2/Me_6$-TREN in hexane, toluene and styrene (Fig. 9b). A surface-disproportionation process takes place in these nonpolar solvents in which the Cu(0) nanoparticles formed coat the CuBr surface, preventing further disproportionation. The extent of surface disproportionation is limited by the solubility of CuBr and $CuBr_2$ in the reaction mixture and/or the ability of the nonpolar solvent to stabilize colloidal Cu(0) nanoparticles.

### Disproportionation of $CuBr/Me_6$-TREN in protic, dipolar aprotic, polar and nonpolar monomers

Inspired by the positive results from the disproportionation of $CuBr/Me_6$-TREN in solvents with different polarity profiles, the disproportionation of CuBr was performed in a diversity of monomers, including acrylates, methacrylates, acrylamide and styrene. Fig. 7a shows that $Me_6$-TREN favors the disproportionation of CuBr in 2-hydroxyethyl acrylate (HEA), 2-hydroxyethyl methacrylate (HEMA), oligo(ethylene oxide) methyl ether acrylate (OEOMEA), oligo(ethylene oxide) methyl ether methacrylate (OEOMA), and *N*,*N*-dimethyl acrylamide (DMA), resulting in the sedimentation of Cu(0) nanoparticles on the bottom of the cuvette and a green or blue color indicating the

 

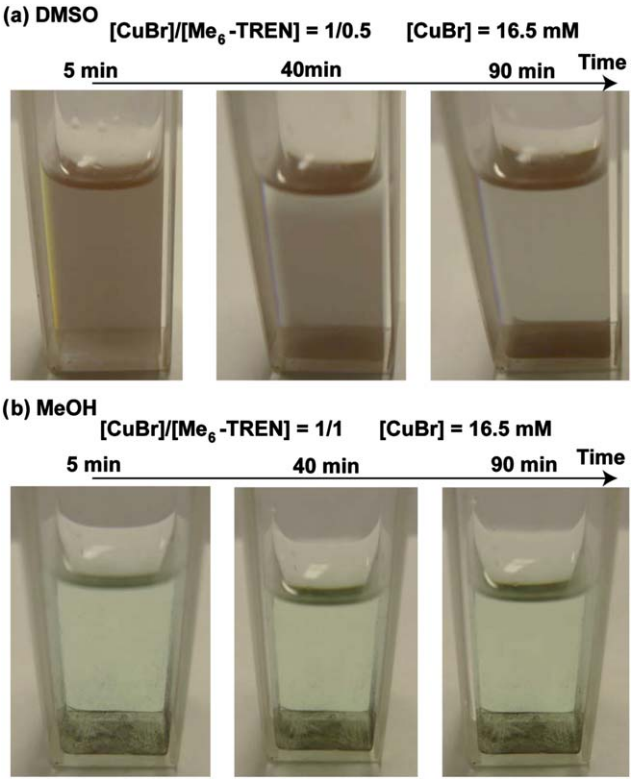


**Fig. 4** Visual observation comparing the stability of Cu(0) nanoparticles generated from the disproportionation of CuBr/$Me_6$-TREN in DMSO (a); and MeOH (b) at 5, 40 and 90 min after mixing the reagents at 25 °C. Conditions: solvent = 1.8 mL, [CuBr] = 16.5 mM, (a) [CuBr]/[$Me_6$-TREN] = 1/0.5 and (b) [CuBr]/[$Me_6$-TREN] = 1/1.

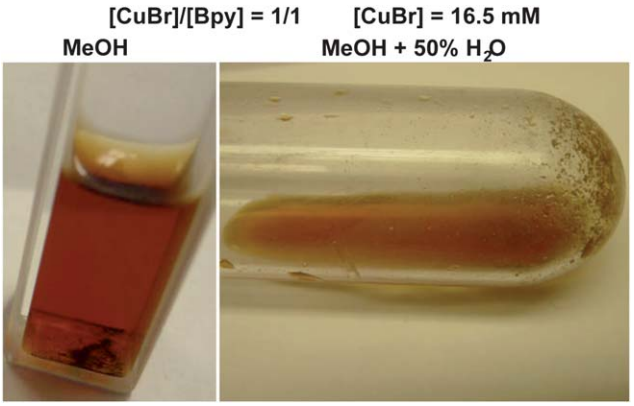


**Fig. 5** Visual observation of the disproportionation of CuBr–bpy in MeOH and MeOH + 50% $H_2O$ at 25 °C. Conditions: solvent = 1.8 mL, [CuBr] = 16.5 mM, [CuBr]/[bpy] = 1/1. Pictures were taken 10 min after mixing the reagents.

formation of soluble $CuBr_2$/$Me_6$-TREN species. The latter was supported by the UV-vis spectra (Fig. 9c). While the disproportionation of CuBr in these polar monomers is expected, it opens up the possibility for bulk polymerization of those monomers *via* SET-LRP.

Unexpectedly, the disproportionation of CuBr into Cu(0) and $CuBr_2$ was observed even in the less polar acrylates and methacrylates monomers. In the acrylate series, it was found that methyl acrylate (MA) mediates the rapid disproportionation of CuBr, generating Cu(0) nanoparticles that agglomerate at the bottom of the UV-vis cuvette. The absorbance of $CuBr_2$/$Me_6$-TREN generated by disproportionation in MA increases over time (Fig. 8a). While ethyl acrylate (EA) promotes the disproportionation process, $CuBr_2$ was not soluble in EA and is observed as a green insoluble salt in the reaction mixture. The extent of disproportionation was lowest in *n*-butyl acrylate (BA), *t*-butyl acrylate (*t*-BA) and 2-ethyl hexyl acrylate (2-EHA) due to the limited solubility of $CuBr_2$/$Me_6$-TREN in these monomers (Fig. 7b). The presence of Cu(0) nanoparticles with no UV-vis absorbance of $CuBr_2$/$Me_6$-TREN in these mixtures suggests a surface disproportionation process in BA, *t*-BA and 2-EHA. The limited solubility of $CuBr_2$ in BA explains why this monomer is more difficult to polymerize using Cu(0)-mediated SET-LRP techniques. In addition, disproportionation of CuBr/$Me_6$-TREN was also observed in methyl methacrylate (MMA), and supported by UV-vis spectroscopy (Fig. 8b). The extent of disproportionation in MMA increases substantially by the addition of DMSO (Fig. 7b).

### Support for visualizations in polar and nonpolar media by UV-vis spectroscopy

In addition to visualization of the disproportionation process, UV-vis spectra were recorded to confirm the formation of the solution of $CuBr_2$/N-ligand complex. The absorbance of $CuBr_2$/$Me_6$-TREN complex can be seen at 957 nm and 742 nm from the UV-vis spectra of the disproportionation mixtures in representative polar protic solvents (Fig. 9a), nonpolar solvents such as anisole and THF (Fig. 9b), polar monomers (Fig. 9c) and nonpolar monomers such as MA and MMA (Fig. 9d). It should be noted that in alcohols the extent of disproportionation decreases with increasing alkyl chain length and with increasing steric hindrance of the alcohol, to a first approximation (Fig. 9a). By contrast, there is no absorbance corresponding to $CuBr_2$/$Me_6$-TREN when nonpolar solvents such as toluene and hexane (Fig. 9b) and when styrene are used as a medium (Fig. 9d) despite the visualization of a surface disproportionation. This confirms the insolubility of $CuBr_2$/$Me_6$-TREN in these reaction media.

### Activation of MBP by Cu(0) nanoparticles generated by disproportionation of CuBr in polar solvents. Visualization of the cooperative and synergistic solvent effects

A previous report from our laboratory demonstrated for the first time the visualization of the SET activation mediated by Cu(0) nanoparticles generated from the disproportionation of CuBr/$Me_6$-TREN in DMSO and MBP initiator.[20] Upon addition of MBP, the Cu(0) nanoparticles were completely consumed within 5 min, demonstrating the extremely reactive nature of the *nascent* Cu(0) nanoparticles. This is in agreement with a previous report demonstrating the unprecedentedly fast SET-LRP of MA catalyzed by mimics of *nascent* Cu(0) powder prepared by disproportionation.[21]

To investigate the reactivity of the Cu(0) nanoparticles formed by disproportionation, the activation of MBP was

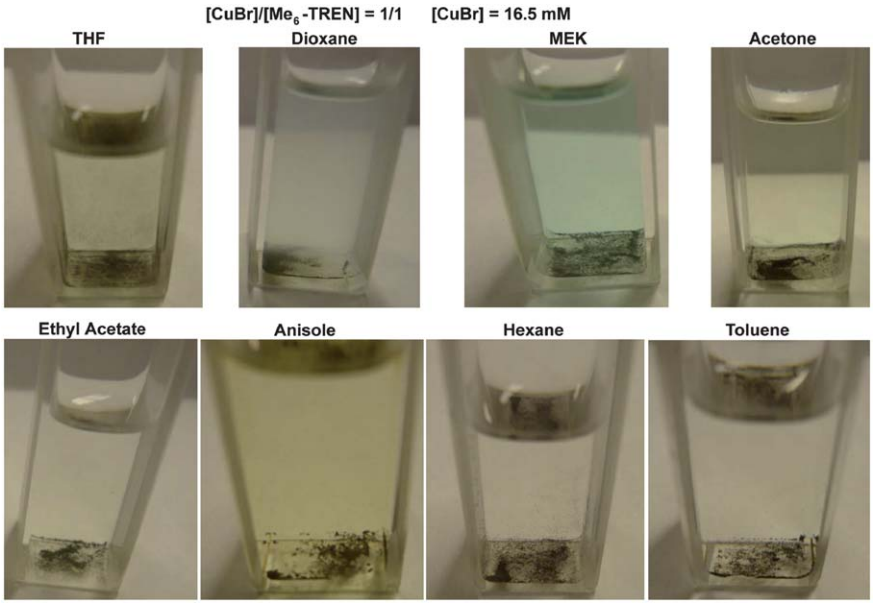


**Fig. 6** Visual observation of Cu(0) nanoparticles generated from the disproportionation of CuBr/$Me_6$-TREN in nonpolar solvents at 25 °C. Conditions: solvent = 1.8 mL, [CuBr] = 16.5 mM, [CuBr]/[$Me_6$-TREN] = 1/1. Pictures were taken 15 min after mixing the reagents.

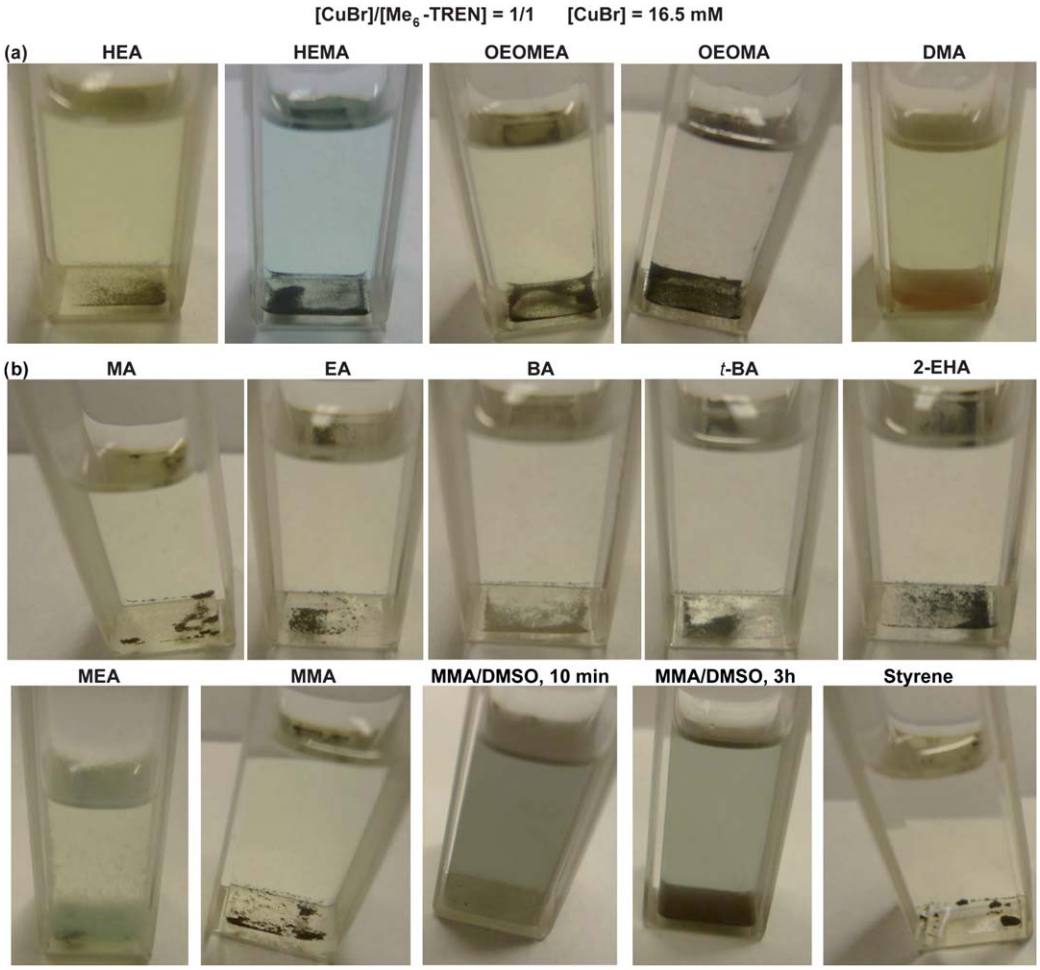


**Fig. 7** Visual observation of Cu(0) nanoparticles generated from the disproportionation of CuBr/$Me_6$-TREN in a range of commercial polar monomers (a); and nonpolar monomers (b) at 25 °C. Conditions: monomer = 1.8 mL, [CuBr] = 16.5 mM, [CuBr]/[$Me_6$-TREN] = 1/1. Pictures were taken 15 min after mixing reagents, except DMA, which was taken 2 h after mixing the reagents.

 

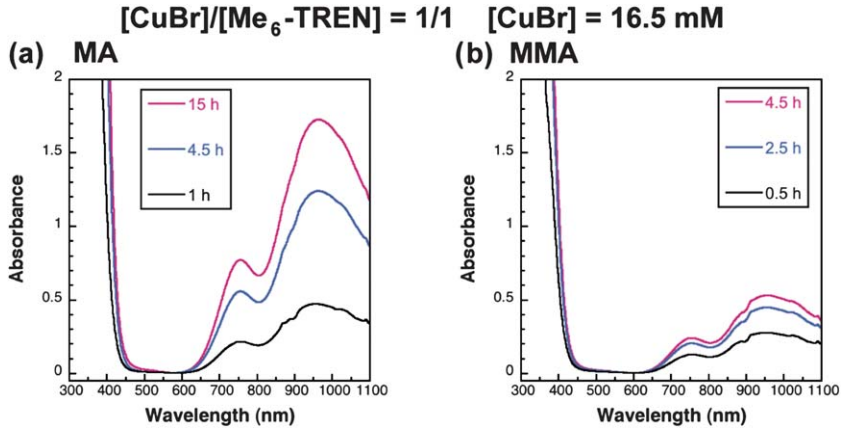


**Fig. 8** UV-vis spectra of the disproportionation of CuBr/$Me_6$-TREN in MA (a); and MMA (b) over time. Conditions: monomer = 1.8 mL, [CuBr] = 16.5 mM, [CuBr]/[$Me_6$-TREN] = 1/1.



performed in a series of organic solvents and solvent mixtures with different polarity profiles. Fig. 10 shows the visual observation of the disproportionation mixture of CuBr/$Me_6$-TREN in DMSO, DMSO + 75% MeOH and MeOH before and after addition of MBP (Fig. 10a–c). Consistent to the previous report, addition of MBP to the disproportionation mixture in DMSO resulted in a rapid consumption of the Cu(0) nanoparticles (Fig. 10a). Similarly, the Cu(0) nanoparticles generated from the disproportionation of CuBr in DMSO + 75% MeOH were consumed within 10 min of the addition of MBP (Fig. 10b). On the other hand, the consumption of Cu(0) nanoparticles generated in MeOH was noticeably slower, reaching completion after 1.5 h (Fig. 10c). This result is in agreement with the comparative rates of the polymerization of MA in these solvents, in which addition of the more polar solvent, MeOH, in DMSO resulted in an increase in $k_p^{app}$, from 0.072 $min^{-1}$ in DMSO to

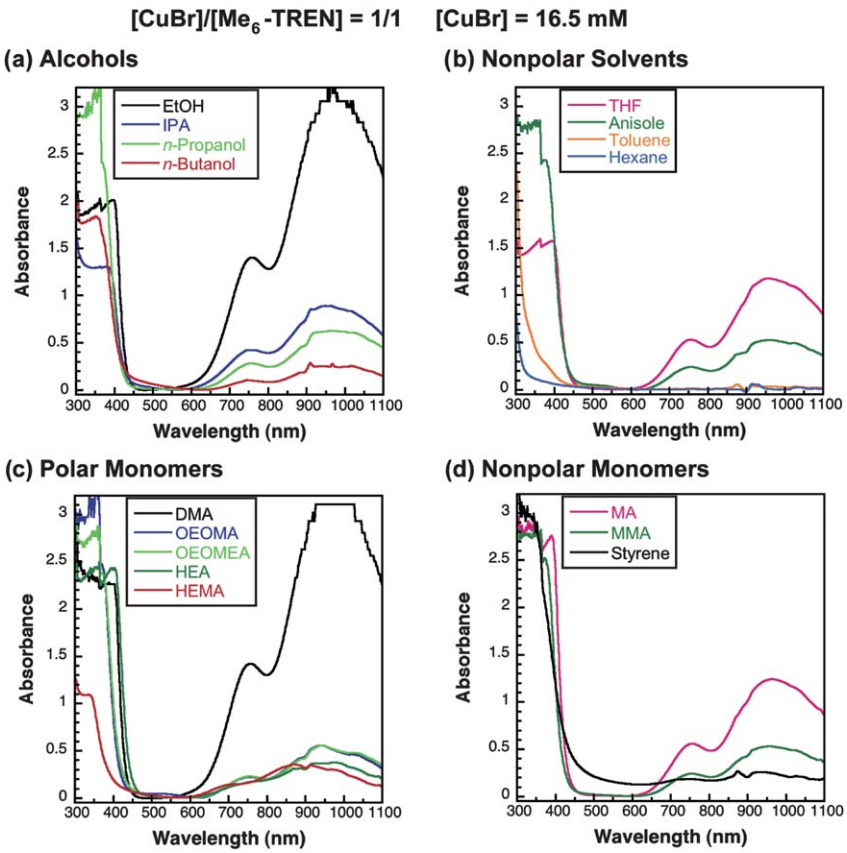


**Fig. 9** UV-vis spectra of the disproportionation of CuBr/$Me_6$-TREN in (a) protic solvents; (b) nonpolar solvents; (c) polar monomers; and (d) nonpolar monomers. Conditions: solvent or monomer = 1.8 mL, [CuBr] = 16.5 mM, [CuBr]/[$Me_6$-TREN] = 1/1.

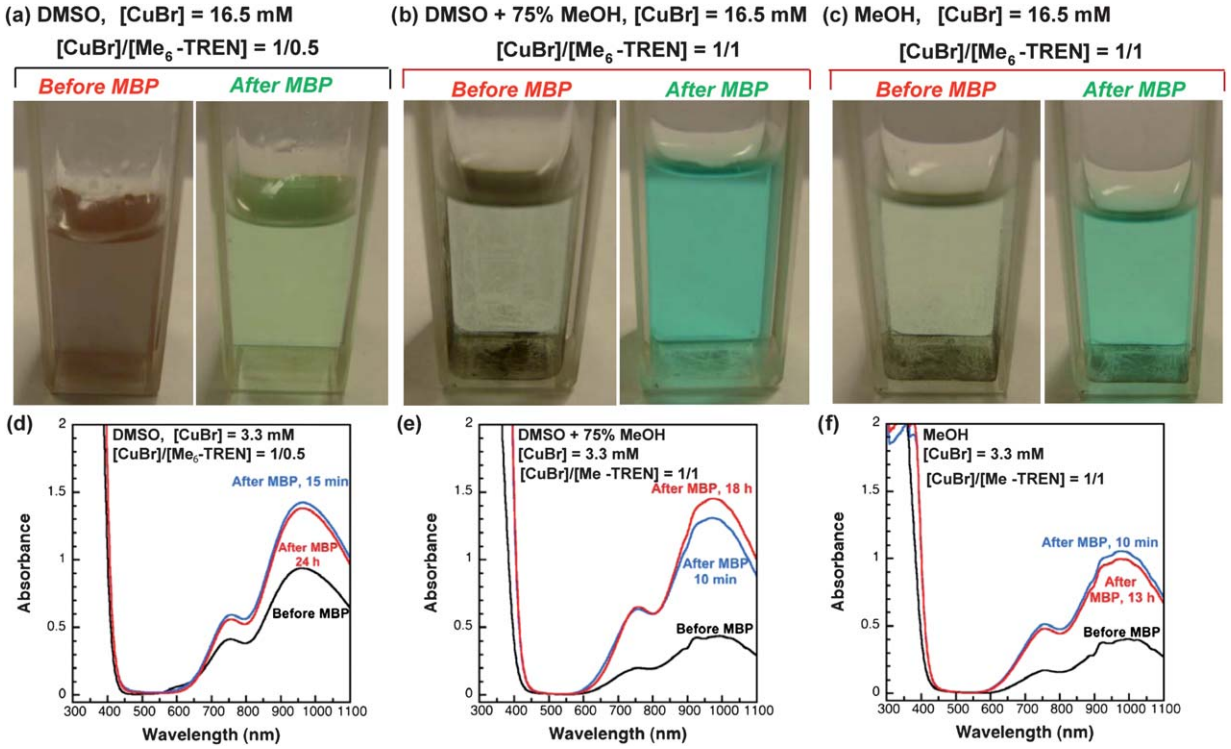


**Fig. 10** Visual observation of Cu(0) nanoparticles and supporting UV-vis spectra of $CuBr_2$ generated from the disproportionation of $CuBr/Me_6$-TREN in DMSO (a and d); DMSO + 75% MeOH (b and e); and MeOH (c and f) before and 10 min after the addition of MBP at 25 °C. Conditions: solvent = 1.8 mL, [MBP]/[CuBr]/[$Me_6$-TREN] = 10/1/0.5 (a and d); [MBP]/[CuBr]/[$Me_6$-TREN] = 10/1/1 (b, c, e and f); [CuBr] = 16.5 mM (a–c); [CuBr] = 3.3 mM (d–f).

0.084 $min^{-1}$ in DMSO + 75% MeOH.[13b] However, $k_p^{app}$ is the slowest in MeOH (0.034 $min^{-1}$), despite its higher polarity and higher ability to disproportionate CuBr.[13b]

The difference in reactivity of these Cu(0) nanoparticles generated in the above solvents can be explained by the ability of some of these solvents such as DMSO to stabilize Cu(0) colloidal nanoparticles, and by decreasing the nucleation and growth processes that is accessible in solvents that provide a higher extent of disproportionation (MeOH, $H_2O$) but no stabilization of the Cu(0) nanoparticles. DMSO is a unique solvent that is relatively polar, promotes extensive disproportionation of CuX, particularly at low ligand levels, and stabilizes Cu(0) colloidal nanoparticles (Fig. 1 and 10a). Since SET activation is a surface-dependent event,[17,20,22] the production of extremely small Cu(0) nanoparticles results in extremely high surface area that allows an accelerated activation of MBP initiator, and therefore, the consumption of these Cu(0) nanoparticles before they nucleate and grow. In MeOH, Cu(0) colloidal nanoparticles are not stabilized. As a consequence, nucleation and growth of larger nanoparticles are favored in MeOH. Ultimately, Cu(0) nanoparticles agglomerate and precipitate in MeOH and $H_2O$, resulting in a lower Cu(0) surface area that does not mediate a fast activation of MBP. As a result, despite being a more polar solvent that disproportionates CuBr to a higher extent than DMSO, the Cu(0)-mediated activation of MBP proceeds at a slower rate in MeOH than in DMSO. The binary mixture of DMSO with 75% MeOH combines both the polar nature of the solvent mixture, the ability to stabilize Cu(0) colloidal nanoparticles, and the higher ability of MeOH to disproportionate CuBr. The activation of MBP by Cu(0) colloidal nanoparticles generated in DMSO containing 75% MeOH, is therefore, faster than in pure MeOH or pure DMSO. In short, *visualization of the comparative stability of Cu(0) colloidal nanoparticles generated by disproportionation in different solvents demonstrates the synergistic solvent effects, in which the kinetics of SET-LRP is determined by the solvent polarity, as well as the ability of the solvent to disproportionate and to stabilize Cu(0) colloidal nanoparticles and control their size*.

The disproportionation of $CuBr/Me_6$-TREN in DMSO, DMSO + 75% MeOH and in MeOH in the presence and absence of an activation process was also monitored by UV-vis spectroscopy (Fig. 10d–f). In this set of experiments, [CuBr] = 3.3 mM was used to prevent saturation of the detector. In all cases, after addition of MBP the concentration of $CuBr_2$ immediately increased due to activation. The reaction mixtures were monitored by UV-vis over the course of several hours. However, no reduction of the absorbance of $CuBr_2/Me_6$-TREN was observed (Fig. 10d–f). This result excludes the possibility of CuBr formed from the reduction of $CuBr_2$ by Cu(0) in the presence of the activation of MBP.[11]

### Activation of MBP by Cu(0) nanoparticles generated by disproportionation of CuBr in nonpolar solvents. Visualization of the solvent effect on the rate of activation by SET

The results reported in this manuscript have shown the unexpected surface disproportionation in nonpolar solvents to

 

generate insoluble Cu(0) nanoparticles, and the disappearance of Cu(0) nanoparticles after addition of MBP provides a visual and qualitative measure of the rate of activation of MBP. Therefore, the disproportionation of CuBr/$Me_6$-TREN was performed in the absence and presence of an activation process with MBP in nonpolar solvents to investigate the effect of the solvent polarity on the rate of SET activation and to gain further mechanistic insight into the reaction process.

In this series of experiments, CuBr was allowed to disproportionate in the nonpolar solvents, toluene and hexane (Fig. 11). After 30 min, MBP (10 equivalent with respect to CuBr concentration) was added to the disproportionation mixtures, and the reactions were monitored over a period of 40 min. The formation of bright green insoluble $CuBr_2$ indicates the reaction between MBP and the Cu(0) occurred. The limited solubility of $CuBr_2$/N-ligand in toluene and hexane has been reported previously.[10e,23] However, a significant proportion of insoluble Cu(0) nanoparticles remained in the UV-vis cuvette even after 40 min following the addition of MBP. This is in contrast with the complete consumption of Cu(0) colloidal nanoparticles generated from the disproportionation process in DMSO upon addition of MBP (Fig. 10a). This result is in agreement with the noticeably slower rate of polymerization of MA in toluene than in DMSO,[24] and demonstrates visually the dependence of the SET process on the nature of solvents.

To further confirm the enhanced rate of SET activation in polar solvents, DMSO was added to the disproportionation mixtures in toluene and hexane 40 min after addition of MBP. After the addition of DMSO, Cu(0) was consumed by activation within 5 min (Fig. 11). A similar trend was observed when MeCN was used as the second solvent (Fig. 12). The consumption of Cu(0) nanoparticles formed from disproportionation in toluene by addition of MeCN was slower than when DMSO was added, reaching completion after 17 min. These visualization experiments confirm the enhanced SET in polar solvents such as DMSO and MeCN, attributable to the stabilization of the polar charge transfer complex between the electron-donor Cu(0) and the electron-acceptor alkyl halide.[25] Solvents that stabilize the polar transition state should also enhance the rate of activation.[5b,25]

## Perspectives of the visualization of the disproportionation process and of the Cu(0)-mediated activation by SET

Understanding the factors that affect the disproportionation of CuX into Cu(0) and $CuX_2$ is critical to the elaboration of SET-LRP methodologies. Here, the visualization experiments demonstrate that N-ligands such as $Me_6$-TREN, TREN and bpy mediate the disproportionation of CuBr in a wide range of commercial solvents and monomers with different polarity profiles. Disproportionation of CuBr in polar monomers including HEA, HEMA, OEOMEA, OEOMA and DMA, and in alcohols and binary mixtures of alcohols and water mediated by $Me_6$-TREN and bpy suggests that the active catalyst in the CuX-catalyzed ATRP of these monomers[26,27] is more likely the extremely reactive *nascent* Cu(0) nanoparticles generated *in situ* by disproportionation. Likewise, many other ATRP conditions involving CuX–bpy in ionic liquid,[28] alcohols, including

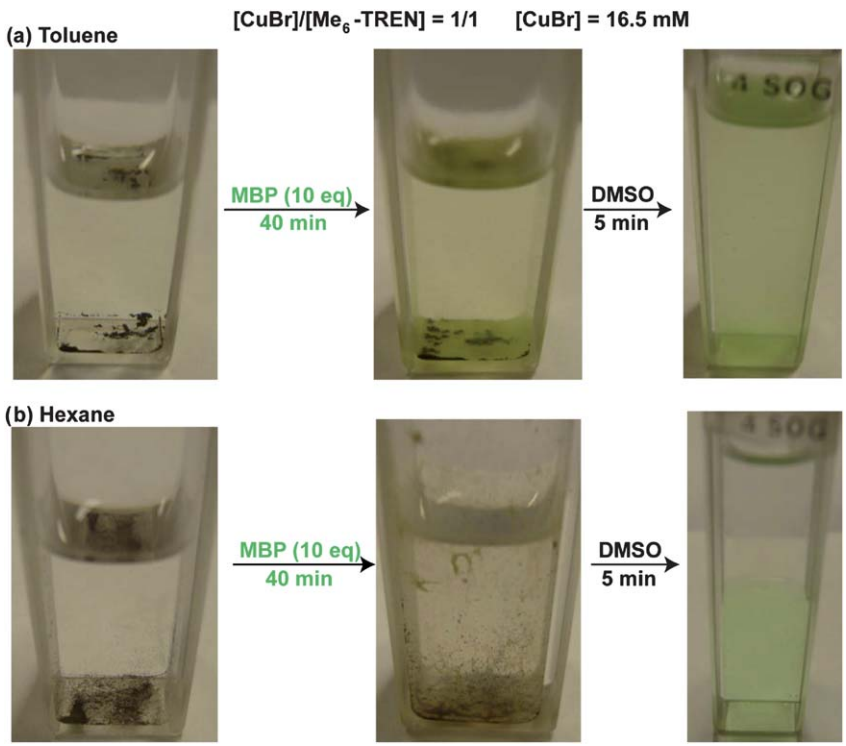


**Fig. 11** Visual observation of Cu(0) nanoparticles and $CuBr_2$ generated from the disproportionation of CuBr in toluene (a); and hexane (b) before and after reaction the with MBP at 25 °C. MBP was added to the disproportionation mixtures after 40 min, followed by addition of 1.8 mL of DMSO. Conditions: solvent = 1.8 mL, [CuBr] = 16.5 mM, [MBP]/[CuBr]/[$Me_6$-TREN] = 10/1/1.

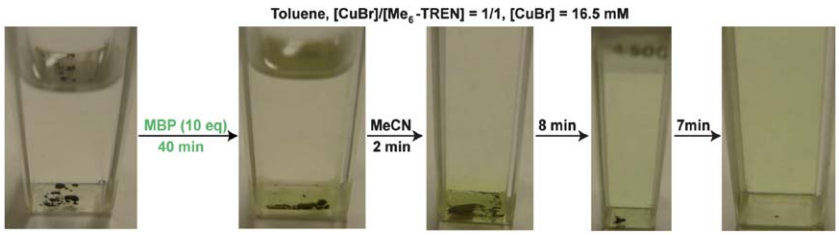


**Fig. 12** Visual observations of Cu(0) nanoparticles and $CuBr_2$ generated from the disproportionation of $CuBr/Me_6$-TREN in toluene before and after the activation with MBP at 25 °C. MBP was added to the disproportionation mixtures after 40 min, followed by addition of 1.8 mL of MeCN. Conditions: toluene = 1.8 mL, [CuBr] = 16.5 mM, [MBP]/[CuBr]/[$Me_6$-TREN] = 10/1/1.



$CF_3CH_2OH$,[28,29] and their binary mixtures with water,[30] and CuX–$Me_6$-TREN in alcohols,[31] ionic liquids,[32] DMSO,[33] DMF and its binary mixtures with water[7,34] promote the disproportionation of CuX to generate the *nascent* Cu(0) activator and the $CuX_2$ deactivator, and therefore, proceed *via* a SET-LRP mechanism.

The unexpected discovery of the disproportionation of $CuBr/Me_6$-TREN in less polar solvents and monomers such as dioxane, anisole, ethyl acetate, acrylates and methacrylates will facilitate the design of experimental conditions for effective SET-LRP of the less polar monomers in solution and even in bulk. One important observation from this series of visualization experiments is that the solubility of $CuX_2$/N-ligand should be taken into consideration when designing SET-LRP reaction conditions. While disproportionation occurs in nonpolar solvents or monomers such as hexane, toluene, dioxane and styrene, the solubility of $CuBr_2/Me_6$-TREN complex in these solvents is limited or negligible, leading to a "surface disproportionation" event. In the context of Cu(0)-mediated polymerization, limited solubility of $CuX_2$/N-ligand or the heterogeneity of the deactivation step would result in inefficient reversible termination of the propagating radicals, leading to increased bimolecular termination. This would explain the progressive loss of chain-end functionality when the Cu(0)-mediated polymerization of MA was performed in the nonpolar solvent toluene,[10e,24] and the limited conversion in the CuX–$Me_6$-TREN catalyzed ATRP in nonpolar solvents. *It is anticipated that improving the solubility of $CuX_2$/N-ligand in nonpolar media would increase the efficiency of the reversible deactivation, allowing for retention of polymer chain-end functionality in SET-LRP of nonpolar monomers*.

The disproportionation of $CuBr/Me_6$-TREN to Cu(0) and $CuBr_2$ and the dependence of SET-mediated activation process on the solvent polarity visually demonstrated in the above series of experiments helps to explain the rate acceleration observed when the CuX-catalyzed ATRP reactions were performed in protic solvents such as $H_2O$,[27,30f,g,31a,34,35] alcohols,[36] and dipolar aprotic solvents including DMSO,[37] DMF[37] and ionic liquid.[18,38] In polar media, disproportionation of CuX generates *in situ* highly reactive *nascent* Cu(0) nanoparticles that undergo rapid activation *via* SET of the alkyl halide initiator or dormant polymer chains, and therefore, are responsible for the observed rate acceleration.

Visualization of the disproportionation of CuX/N-ligand provides an efficient method to evaluate combinations of ligands and solvents that promote the disproportionation of CuX, and therefore, mediate effective SET-LRP of monomers with different polarity profiles. This model reaction, in combination with the visualization of the SET activation of alkyl halide initiator by *nascent* Cu(0) nanoparticles enable rapid discrimination between SET-LRP, in which both the catalytically active Cu(0) activator and $CuX_2$ deactivator are generated *in situ* by disproportionation, and ATRP in which no disproportionation of CuX occurs.

## Conclusions

This article demonstrates that $CuX_2$-stabilizing N-ligands such as $Me_6$-TREN, TREN and bpy can disproportionate CuBr in a wide diversity of polar solvents and monomers. Unexpectedly, insoluble Cu(0) nanoparticles were generated also in nonpolar solvents and nonpolar monomers as visually observed. The Cu(0) nanoparticles generated from the disproportionation in DMSO are more stable than those generated in MeOH, and this result has been used to explain why SET-LRP performed in DMSO solvent exhibits a faster SET-LRP rate than in MeOH despite the latter being more polar and producing a larger extent of disproportionation. This combination of effects also explains the synergistic mixed solvent effect in these combinations of solvents. When disproportionation is performed in polar solvents and polar monomers a solution disproportionation occurs, with soluble $CuBr_2$ formed. When nonpolar solvents and nonpolar monomers are used, a surface disproportionation occurs and green insoluble $CuBr_2$ is observed on the base of the UV-vis cuvette. Since *nascent* Cu(0) nanoparticles are highly reactive, and since $CuBr_2$ is responsible for deactivation in SET-LRP, these results have been used to explain the rate acceleration previously observed during ATRP reactions performed in polar solvents, and the loss of functionality presently observed during SET-LRP and ATRP reactions performed in nonpolar solvents.

The comparative rate of activation in DMSO, MeCN and toluene has been demonstrated qualitatively by visualizing the loss of insoluble particles after the addition of MBP to the Cu(0) generated by disproportionation. It was shown that *nascent* Cu(0) nanoparticles are the activating species, and that there is no reduction of $CuBr_2$ by Cu(0) during the activation to form CuX on the timescale of a polymerization reaction. Finally, it was shown that polar solvents catalyze the reaction between nascent Cu(0) and MBP, indicating a polar transition state for

 

the activation process in this reaction. The visualization methodology elaborated here will have significant implications for the rapid discrimination between SET-LRP and ATRP and for the elaboration of SET-LRP conditions demanded by the synthesis of well-defined polymers with complex architecture.

## Experimental

### Reagents

All solvents were used as received except DMSO, which was distilled over $CaH_2$ before use and stored in a glovebox. All monomers were purified by passing through a short column of basic alumina to remove inhibitor before use. Methyl 2-bromopropionate (MBP) (Acros, 99%), tris(2-aminoethyl)amine (TREN) (Acros, 96%), 2,2-bipyridine (bpy) (Aldrich, 99%) were used as received. CuBr was prepared by the reduction of $CuBr_2$ according to a literature procedure[15] and stored in the glovebox before use. Tris[2-(dimethylamino)ethyl]amine ($Me_6$-TREN) was synthesized and purified according to a literature procedure.[39] 1-Butyl-3-methylimidazolium hexafluorophosphate ($bmimPF_6$) was synthesized according to a literature procedure.[18]

DMSO, methyl methacrylate (MMA), methanol (MeOH), ethylene glycol, *N*,*N*-dimethylformamide (DMF), acetonitrile (MeCN), tetrahydrofuran (THF), acetone, hexane and toluene were purchased from Fisher and were used as received. *n*-Propanol, isopropanol, *n*-butanol (*n*-BuOH), *t*-butanol (*t*-BuOH), *n*-octanol, diethylene glycol, propylene carbonate (PC), methyl acrylate (MA), ethyl acrylate (EA), butyl acrylate (BA), *t*-butyl acrylate (*t*-BA), 2-hydroxyethyl methacrylate (HEMA), oligo(ethylene oxide) methyl ether acrylate (OEOMEA), oligo(ethylene oxide) methyl ether methacrylate (OEOMA) and *N*,*N*-dimethyl acrylamide (DMA) were purchased from Sigma-Aldrich and were used as received. Ethanol (EtOH, 95%), benzyl alcohol (BnOH), 2,2,2-trifluoroethanol ($CF_3CH_2OH$), hexafluoroisopropanol ($(CF_3)_2CHOH$), methyl ethyl ketone (MEK), 2-hydroxyethyl acrylate (HEA) and 2-ethyl hexyl acrylate (2-EHA) were purchased from Acros and were used as received. Styrene was purchased from Lancaster and was used as received.

### Instrumentation

Disproportionation experiments were performed in 3.5 mL volume Starna UV-vis quartz cuvettes with airtight screw cap fitting. The glovebox was an Innovative Technology Inc. model operating under a nitrogen atmosphere, deoxygenated with a copper catalyst and with moisture level ideally maintained below 25 ppm. For best results the glovebox was purged immediately before disproportionation experiments were performed. Photographs were taken with a digital camera using a white background. UV-vis spectra were recorded on a Shimadzu 1601 spectrometer with Shimadzu UV-Probe software.

**Typical procedure for disproportionation in solvents and monomers at [CuBr]/[$Me_6$-TREN] = 1/1 mole ratio.** $Me_6$-TREN and MBP were deoxygenated by bubbling with nitrogen for one hour in a Schlenk tube and transferred into the glovebox. Two microsyringes were kept in the glovebox to handle the ligand and MBP initiator. CuBr (4.3 mg, 0.03 mmol) was measured into a UV cuvette and carefully transferred into the glovebox. Separately, the disproportionation medium (solvent or monomer) was deoxygenated either by bubbling with nitrogen for one hour, by six cycles of freeze–pump–thaw from a dry ice/acetone bath or liquid nitrogen, and transferred into the glovebox. Inside the glovebox, 1.8 mL of solvent was delivered into the cuvette containing CuBr using a disposable 3 mL plastic syringe, followed by the addition of 8 μL of $Me_6$-TREN (6.8 mg, 0.03 mmol) to achieve [CuBr] = [$Me_6$-TREN] = 16.5 mM. The cuvette was shaken and removed from the glovebox, and the reagents were mixed by 1–2 min vortex. Photographs were taken at different times throughout the reactions. As an alternative procedure, the disproportionation medium and the ligand could be prepared as a stock solution and degassed together outside the glovebox before addition to the CuBr in the cuvette. For activation of Cu(0) nanoparticles, the cuvette was returned to the glovebox and MBP (50.2 mg, 35 μL, 0.3 mmol) was added by a microsyringe.

**Disproportionation of CuBr/$Me_6$-TREN in water.** This experiment was performed outside of the glovebox due to concern with introduction of moisture in the dry glovebox. Therefore, two Schlenk tubes were connected. Deionized water was purged with nitrogen in a Schlenk tube for one hour, and then $Me_6$-TREN was added to the water. After five further minutes purging, a second Schlenk tube containing CuBr was attached while a nitrogen atmosphere was maintained. Water was decanted by rapid tilting onto the connected Schlenk tube containing CuBr to start the disproportionation.

**Effect of oxygen on reproducibility.** The disproportionation reactions are particularly sensitive to oxygen. In the presence of traces of oxygen, the disproportionation mixture turned green/blue corresponding to the formation of $CuBr_2$/N-ligand complex in solution, but the Cu(0) colloidal particles were not generated. This indicates the oxidation of soluble CuBr/N-ligand in the presence of oxygen. Therefore, thorough deoxygenation of reagents and a well-maintained glovebox are important factors when performing the disproportionation reactions. The disproportionation of CuBr/$Me_6$-TREN in MeCN, in which no Cu(0) was observed, was repeated four times before being considered valid.

## Acknowledgements

Financial support by the National Science Foundation (DMR-1120901, DMR-1066116) and the P. Roy Vagelos Chair at Penn are gratefully acknowledged.

## Notes and references

1 A. D. Asandei and V. Percec, *J. Polym. Sci., Part A: Polym. Chem.*, 2001, **39**, 3392–3418.
2 J. Queffelec, S. G. Gaynor and K. Matyjaszewski, *Macromolecules*, 2000, **33**, 8629–8639.
3 (*a*) H. Fischer, *J. Polym. Sci., Part A: Polym. Chem.*, 1999, **37**, 1885–1901; (*b*) H. Fischer, *Chem. Rev.*, 2001, **101**, 3581–3610.
4 (*a*) V. Percec, A. V. Popov, E. Ramirez-Castillo, M. Monteiro, B. Barboiu, O. Weichold, A. D. Asandei and C. M. Mitchell,

*J. Am. Chem. Soc.*, 2002, **124**, 4940–4941; (*b*) V. Percec, A. V. Popov, E. Ramirez-Castillo and O. Weichold, *J. Polym. Sci., Part A: Polym. Chem.*, 2003, **41**, 3283–3299.

5 (*a*) V. Percec, T. Guliashvili, J. S. Ladislaw, A. Wistrand, A. Stjerndahl, M. J. Sienkowska, M. J. Monteiro and S. Sahoo, *J. Am. Chem. Soc.*, 2006, **128**, 14156–14165; (*b*) B. M. Rosen and V. Percec, *Chem. Rev.*, 2009, **109**, 5069–5119.

6 (*a*) G. Lligadas and V. Percec, *J. Polym. Sci., Part A: Polym. Chem.*, 2007, **45**, 4684–4695; (*b*) E. Nicol, T. Derouineau, F. Puaud and A. Zaitsev, *J. Polym. Sci., Part A: Polym. Chem.*, 2012, **50**, 3885–3894; (*c*) N. H. Nguyen, J. Kulis, H.-J. Sun, Z. Jia, B. van Beusekom, M. E. Levere, D. A. Wilson, M. J. Monteiro and V. Percec, *Polym. Chem.*, 2013, **4**, 144–155.

7 (*a*) C. Feng, Z. Shen, L. Gu, S. Zhang, L. Li, G. Lu and X. Huang, *J. Polym. Sci., Part A: Polym. Chem.*, 2008, **46**, 5638–5651; (*b*) C. Feng, Z. Shen, Y. Li, L. Gu, Y. Zhang, G. Lu and X. Huang, *J. Polym. Sci., Part A: Polym. Chem.*, 2009, **47**, 1811–1824.

8 N. H. Nguyen, B. M. Rosen and V. Percec, *J. Polym. Sci., Part A: Polym. Chem.*, 2010, **48**, 1752–1763.

9 (*a*) S. Fleischmann and V. Percec, *J. Polym. Sci., Part A: Polym. Chem.*, 2010, **48**, 2251–2255; (*b*) S. Fleischmann and V. Percec, *J. Polym. Sci., Part A: Polym. Chem.*, 2010, **48**, 4884–4888.

10 (*a*) C. Boyer, A. H. Soeriyadi, P. B. Zetterlund and M. R. Whittaker, *Macromolecules*, 2011, **44**, 8028–8033; (*b*) F. Nyström, A. H. Soeriyadi, C. Boyer, P. B. Zetterlund and M. R. Whittaker, *J. Polym. Sci., Part A: Polym. Chem.*, 2011, **49**, 5313–5321; (*c*) A. H. Soeriyadi, C. Boyer, F. Nystrom, P. B. Zetterlund and M. R. Whittaker, *J. Am. Chem. Soc.*, 2011, **133**, 11128–11131; (*d*) C. Boyer, A. Derveaux, P. B. Zetterlund and M. R. Whittaker, *Polym. Chem.*, 2012, **3**, 117–123; (*e*) N. H. Nguyen, M. E. Levere, J. Kulis, M. J. Monteiro and V. Percec, *Macromolecules*, 2012, **45**, 4606–4622; (*f*) N. H. Nguyen, M. E. Levere and V. Percec, *J. Polym. Sci., Part A: Polym. Chem.*, 2012, **50**, 860–873.

11 M. E. Levere, N. H. Nguyen and V. Percec, *Macromolecules*, 2012, **45**, 8267–8274.

12 (*a*) J. M. Ottino, *AIChE J.*, 2003, **49**, 292–299; (*b*) J. M. Ottino, *Nature*, 2004, **427**, 399.

13 (*a*) N. H. Nguyen, B. M. Rosen, X. Jiang, S. Fleischmann and V. Percec, *J. Polym. Sci., Part A: Polym. Chem.*, 2009, **47**, 5577–5590; (*b*) X. Jiang, S. Fleischmann, N. H. Nguyen, B. M. Rosen and V. Percec, *J. Polym. Sci., Part A: Polym. Chem.*, 2009, **47**, 5591–5605.

14 (*a*) B. M. Rosen and V. Percec, *J. Polym. Sci., Part A: Polym. Chem.*, 2007, **45**, 4950–4964; (*b*) N. H. Nguyen, X. Jiang, S. Fleischmann, B. M. Rosen and V. Percec, *J. Polym. Sci., Part A: Polym. Chem.*, 2009, **47**, 5629–5638; (*c*) N. H. Nguyen, M. E. Levere and V. Percec, *J. Polym. Sci., Part A: Polym. Chem.*, 2012, **50**, 35–46.

15 B. M. Rosen, X. Jiang, C. J. Wilson, N. H. Nguyen, M. J. Monteiro and V. Percec, *J. Polym. Sci., Part A: Polym. Chem.*, 2009, **47**, 5606–5628.

16 (*a*) F. Fenwick, *J. Am. Chem. Soc.*, 1926, **48**, 860–870; (*b*) G. W. Tindall and S. Bruckenstein, *Anal. Chem.*, 1968, **40**, 1402–1404; (*c*) S. Ahrland and J. Rawsthorne, *Acta Chem. Scand.*, 1970, **24**, 157–172; (*d*) v. L. Ciavatta, D. Ferri and R. Palombari, *J. Inorg. Nucl. Chem.*, 1980, **42**, 593–598.

17 G. Lligadas, B. M. Rosen, C. A. Bell, M. J. Monteiro and V. Percec, *Macromolecules*, 2008, **41**, 8365–8371.

18 V. Percec and C. Grigoras, *J. Polym. Sci., Part A: Polym. Chem.*, 2005, **43**, 5609–5619.

19 M. J. Monteiro, T. Guliashvili and V. Percec, *J. Polym. Sci., Part A: Polym. Chem.*, 2007, **45**, 1835–1847.

20 M. E. Levere, N. H. Nguyen, H.-J. Sun and V. Percec, *Polym. Chem.*, 2013, DOI: 10.1039/C2PY20791E.

21 X. Jiang, B. M. Rosen and V. Percec, *J. Polym. Sci., Part A: Polym. Chem.*, 2010, **48**, 403–409.

22 N. H. Nguyen, B. M. Rosen, G. Lligadas and V. Percec, *Macromolecules*, 2009, **42**, 2379–2386.

23 Y. Fu, A. Mirzaei, M. F. Cunningham and R. A. Hutchinson, *Macromol. React. Eng.*, 2007, **1**, 425–439.

24 G. Lligadas and V. Percec, *J. Polym. Sci., Part A: Polym. Chem.*, 2008, **46**, 6880–6895.

25 J. F. Bunnett, R. G. Scamehorn and R. P. Traber, *J. Org. Chem.*, 1976, **41**, 3677–3682.

26 (*a*) S. Coca, C. B. Jasieczek, K. L. Beers and K. Matyjaszewski, *J. Polym. Sci., Part A: Polym. Chem.*, 1998, **36**, 1417–1424; (*b*) K. L. Beers, S. Boo, S. G. Gaynor and K. Matyjaszewski, *Macromolecules*, 1999, **32**, 5772–5776; (*c*) J. K. Oh, K. Min and K. Matyjaszewski, *Macromolecules*, 2006, **39**, 3161–3167; (*d*) A. Simakova, S. E. Averick, D. Konkolewicz and K. Matyjaszewski, *Macromolecules*, 2012, **45**, 6371–6379.

27 (*a*) K. L. Robinson, M. A. Khan, M. V. de Paz Banez, X. S. Wang and S. P. Armes, *Macromolecules*, 2001, **34**, 3155–3158; (*b*) X. S. Wang, S. F. Lascelles, R. A. Jackson and S. P. Armes, *Chem. Commun.*, 1999, 1817–1818; (*c*) X. S. Wang and S. P. Armes, *Macromolecules*, 2000, **33**, 6640–6647.

28 (*a*) Y. Terayama, M. Kikuchi, M. Kobayashi and A. Takahara, *Macromolecules*, 2011, **44**, 104–111; (*b*) M. Kobayashi, M. Terada, Y. Terayama, M. Kikuchi and A. Takahara, *Macromolecules*, 2010, **43**, 8409–8415; (*c*) M. Kobayashi, M. Terada, Y. Terayama, M. Kikuchi and A. Takahara, *Isr. J. Chem.*, 2012, **52**, 364–374.

29 M. Kobayashi, M. Terada and A. Takahara, *Soft Matter*, 2011, **7**, 5717–5722.

30 (*a*) M. Kobayashi, M. Terada and A. Takahara, *Faraday Discuss.*, 2012, **156**, 403–412; (*b*) M. Kobayashi and A. Takahara, *Chem. Rec.*, 2010, **10**, 208–216; (*c*) M. Kobayashi, Y. Terayama, H. Yamaguchi, M. Terada, D. Murakami, K. Ishihara and A. Takahara, *Langmuir*, 2012, **28**, 7212–7222; (*d*) D. M. Jones, J. R. Smith, W. T. S. Huck and C. Alexander, *Adv. Mater.*, 2002, **14**, 1130–1134; (*e*) S. Tugulu, R. l. Barbey, M. Harms, M. Fricke, D. Volkmer, A. Rossi and H.-A. Klok, *Macromolecules*, 2007, **40**, 168–177; (*f*) V. L. Osborne, D. M. Jones and W. T. S. Huck, *Chem. Commun.*, 2002, 1838–1839; (*g*) W. Huang, J.-B. Kim, M. L. Bruening and G. L. Baker, *Macromolecules*, 2002, **35**, 1175–1179; (*h*) R. Barbey, L. Lavanant, D. Paripovic, N. Schuwer, C. Sugnaux, S. Tugulu and H.-A. Klok, *Chem. Rev.*, 2009, **109**, 5437–5527.

 

31 (*a*) J. T. Rademacher, M. Baum, M. E. Pallack, W. J. Brittain and W. J. Simonsick, *Macromolecules*, 2000, **33**, 284–288; (*b*) J. Ye and R. Narain, *J. Phys. Chem. B*, 2009, **113**, 676–681.
32 H. Yamaguchi, M. Kikuchi, M. Kobayashi, H. Ogawa, H. Masunaga, O. Sakata and A. Takahara, *Macromolecules*, 2012, **45**, 1509–1516.
33 K. L. Heredia, Z. P. Tolstyka and H. D. Maynard, *Macromolecules*, 2007, **40**, 4772–4779.
34 L. G. V. C. Giancarlo Masci, *Macromol. Rapid Commun.*, 2004, **25**, 559–564.
35 (*a*) X. S. Wang, R. A. Jackson and S. P. Armes, *Macromolecules*, 2000, **33**, 255–257; (*b*) F. Zeng, Y. Shen, S. Zhu and R. Pelton, *J. Polym. Sci., Part A: Polym. Chem.*, 2000, **38**, 3821–3827.
36 (*a*) E. J. Lobb, I. Ma, N. C. Billingham, S. P. Armes and A. L. Lewis, *J. Am. Chem. Soc.*, 2001, **123**, 7913–7914; (*b*) S. McDonald and S. P. Rannard, *Macromolecules*, 2001, **34**, 8600–8602; (*c*) S. M. Kimani and S. C. Moratti, *J. Polym. Sci., Part A: Polym. Chem.*, 2005, **43**, 1588–1598.
37 (*a*) V. Percec, T. Guliashvili, A. V. Popov and E. Ramirez-Castillo, *J. Polym. Sci., Part A: Polym. Chem.*, 2005, **43**, 1935–1947; (*b*) V. Percec, T. Guliashvili, A. V. Popov, E. Ramirez-Castillo and L. A. Hinojosa-Falcon, *J. Polym. Sci., Part A: Polym. Chem.*, 2005, **43**, 1660–1669; (*c*) V. Percec, T. Guliashvili, A. V. Popov, E. Ramirez-Castillo, J. F. J. Coelho and L. A. Hinojosa-Falcon, *J. Polym. Sci., Part A: Polym. Chem.*, 2005, **43**, 1649–1659; (*d*) D. Bontempo, R. C. Li, T. Ly, C. E. Brubaker and H. D. Maynard, *Chem. Commun.*, 2005, 4702–4704; (*e*) S. Monge, V. Darcos and D. M. Haddleton, *J. Polym. Sci., Part A: Polym. Chem.*, 2004, **42**, 6299–6308.
38 (*a*) P. Kubisa, *Prog. Polym. Sci.*, 2004, **29**, 3–12; (*b*) P. Kubisa, *J. Polym. Sci., Part A: Polym. Chem.*, 2005, **43**, 4675–4683.
39 M. Ciampolini and N. Nardi, *Inorg. Chem.*, 1966, **5**, 41–44.